AGU PUBLICATIONS

Geophysical Research Letters

RESEARCH LETTER
10.1002/2016GL069071

Key Points:
- Total pCO_2 trends are spatially variable and controlled by biology
- Anthropogenic CO_2 uptake and trends are controlled by physics
- Spatial variability can lead to extremes in acidification

Supporting Information:
- Supporting Information S1

Correspondence to:
A. Tagliabue,
a.tagliabue@liverpool.ac.uk

Citation:
Tagliabue, A., and K. R. Arrigo (2016), Decadal trends in air-sea CO_2 exchange in the Ross Sea (Antarctica), *Geophys. Res. Lett.*, *43*, doi:10.1002/2016GL069071.

Received 15 APR 2016
Accepted 9 MAY 2016
Accepted article online 11 MAY 2016

Decadal trends in air-sea CO_2 exchange in the Ross Sea (Antarctica)

Alessandro Tagliabue[1] and Kevin R. Arrigo[2]

[1]Department of Earth, Ocean and Ecological Sciences, School of Environmental Sciences, University of Liverpool, Liverpool, UK, [2]Department of Earth System Science, Stanford University, Stanford, California, USA

Abstract Highly productive Antarctic shelf systems, like the Ross Sea, play important roles in regional carbon budgets, but the drivers of local variations are poorly quantified. We assess the variability in the Ross Sea carbon cycle using a regional physical-biogeochemical model. Regionally, total partial pressure of CO_2 (pCO_2) increases are largely controlled by the biological pump and broadly similar to those in the offshore Southern Ocean. However, this masks substantial local variability within the Ross Sea, where interannual fluctuations in total pCO_2 are driven by the biological pump and alkalinity, whereas those for anthropogenic pCO_2 are related to physical processes. Overall, the high degree of spatial variability in the Ross Sea carbon cycle causes extremes in aragonite saturation that can be as large as long-term trends. Therefore, Antarctic shelf polynya systems like the Ross Sea will be strongly affected by local processes in addition to larger-scale phenomena.

1. Introduction

The ocean acts as a sink for atmospheric CO_2 via the solubility and biological pumps [*Volk and Hoffert*, 1985]. The solubility pump is driven by greater solubility of CO_2 at low temperatures that increases CO_2 uptake in cold surface waters, which can then be mixed into the ocean interior away from the air-sea interface. The biological pump is driven by the consumption of CO_2 during photosynthesis by phytoplankton and the subsequent sinking and remineralization of organic carbon at depth. In addition, as alkalinity also affects the partial pressure of seawater CO_2 (pCO_2) via carbon chemistry, with reductions in alkalinity raising ocean pCO_2 (and vice versa), variations in alkalinity can also modify air-sea CO_2 exchange [*Zeebe and Wolf-Gladrow*, 2001]. Atmospheric CO_2 levels are increasing annually due to fossil fuel combustion, cement production, and land use change. The ocean uptake of total CO_2 (including natural and anthropogenic components) by both the solubility and biological pumps drives "ocean acidification," which lowers pH and carbonate ion concentrations, affecting the success of calcite- and aragonite-secreting marine organisms [*Orr et al.*, 2005]. Understanding the rates and drivers of ocean CO_2 uptake are therefore important in understanding the wider carbon cycle implications and the local impacts on vulnerable plankton groups. In that regard, the contribution of anthropogenic CO_2 is often isolated from that of total CO_2 to assess their relative contributions [*Khatiwala et al.*, 2009; *Sallée et al.*, 2012]. By better evaluating the driving mechanisms of changes to the carbon cycle, we can better understand past variations from a mechanistic standpoint and project future changes with more confidence.

Coastal regions around Antarctica such as the Ross Sea are important sites of air-sea CO_2 exchange due to both the solubility and biological pumps. The formation of cold and dense Antarctic Bottom Water in winter [*Gordon et al.*, 2004] is able to transfer CO_2 to the ocean interior. The Ross Sea is also typified by high levels of primary productivity in summer [*Arrigo and van Dijken*, 2003], which depletes CO_2 [*Sweeney*, 2003] and transfers organic carbon to the deep ocean [*Dunbar et al.*, 1998]. Previous work has found that the uptake of anthropogenic CO_2 by the Ross Sea is equivalent to over one quarter of the Southern Ocean uptake [*Arrigo et al.*, 2008b]. Nevertheless, the seasonal formation of sea ice and deep winter entrainment may restrict the Ross Sea CO_2 sink from achieving full atmospheric equilibrium [*McNeil et al.*, 2010].

The Ross Sea has experienced a substantial degree of interannual variation over recent decades due to the calving of icebergs and wider climate anomalies (such as El Niño and the Southern Annular Mode, SAM) [*Arrigo and van Dijken*, 2004; *Martin et al.*, 2007; *Stammerjohn et al.*, 2008]. The SAM affects westerly winds across the Southern Ocean, and although its variability from year to year has emerged as a key driver of Southern Ocean air-sea CO_2 fluxes [*Le Quere et al.*, 2007; *Lenton et al.*, 2009], recent accelerations in CO_2 uptake are not as clearly linked to the SAM [*Landschutzer et al.*, 2015]. In the Ross Sea, remote sensing

suggests links between average chlorophyll *a*, primary production and sea surface temperature, and the SAM index, with on-off shelf contrasts [*Schine et al*., 2016]. A regional modeling study found that The Ross Sea CO_2 sink exhibited a twentyfold variation over the period 1997–2003 when each year was considered discretely [*Arrigo and Van Dijken*, 2007]. Although there is an emerging understanding of the response of the wider Southern Ocean carbon cycle on interannual timescales [*Landschutzer et al*., 2015], the response of Antarctic continental shelf regions including the Ross Sea is poorly understood [*Lenton et al*., 2012]. An improved understanding of what drives the magnitude of the Ross Sea CO_2 sink and its interannual variation would help constrain its future evolution and contribution to regional CO_2 sinks and local acidification. Using a regional ocean model that accounts for the biogeochemistry and carbon cycling of the Ross Sea, we examine the role played by atmospheric and ocean processes in regulating different components of the Ross Sea carbon cycle. In particular, we focus on the role of different external forcings (air temperature, humidity, wind, and sea ice) and ocean properties (primary production, mixed layer depth, sea surface temperature, and alkalinity) in driving the accumulation of anthropogenic carbon and spatial anomalies in both total and anthropogenic pCO_2.

2. Methods

For this study we used the CIAO model as described previously [*Arrigo et al*., 2003]. The physics of CIAO is based on the primitive equation Princeton Ocean Model [*Blumberg and Mellor*, 1987], where vertical mixing includes a turbulence closure scheme [*Mellor and Yamada*, 1982]. CIAO is a σ coordinate model in the vertical dimension and uses a curvilinear coordinate system in the horizontal dimensions with a spatial resolution of approximately 25 km in the southwestern Ross Sea that is the focus of this study. The full spatial domain of CIAO encompasses the region from 135°E to 60°W and 58°S to 78°S (Figure 1a), with climatological boundary conditions [*Arrigo et al*., 2003]. Of particular relevance here, the model carbon system accounts for total dissolved inorganic carbon and dissolved organic carbon. The pCO_2 and pH are computed following the Ocean Carbon Model Intercomparison Project (OCMIP) protocols using an iterative scheme [*Tagliabue and Arrigo*, 2005]. Air-sea CO_2 exchange depends on the air-sea CO_2 gradient, pCO_2 solubility, the Schmidt number for CO_2, the square of the wind speed, and the proportion of a model grid cell that is ice covered. We refer readers to *Tagliabue and Arrigo* [2005] for full details. Alkalinity is modeled as an empirical function of salinity and temperature [*Lee et al*., 2006] and thus does not account for any calcification or calcium carbonate dissolution processes.

After spinning up CIAO for 20 years using climatological forcing, we ran a continuous interannual simulation from 1980 to 2013 using reanalysis products to force the model. Specifically, we took 6-hourly air temperature, specific humidity, sea level pressure, cloud cover, zonal (*U*) and meridional (*V*) component winds, and precipitable water from the National Centers for Environmental Prediction-Department of Energy (NCEP-DOE) Reanalysis 2. Daily sea ice concentrations were taken from the NOAA/National Snow and Ice Data Center Climate Data Record of Passive Microwave Sea Ice [*Peng et al*., 2013]. Sea ice data are incomplete for the early part of the record (1980–1990). Where data are missing, we linearly interpolated. The model was then run from 1980 to 2013 with a time-evolving atmospheric CO_2 concentration from the historical record [*Dlugokencky and Tans*, 2013]. Three additional simulations were also conducted. The first held atmospheric CO_2 constant at its 1980 concentration, and the second and third switched off biological activity, but with fixed and rising atmospheric CO_2, respectively. By comparing the runs with and without time-evolving CO_2 concentrations, we can extract the anthropogenic CO_2 signal (by subtracting one from the other). Due to the greater accuracy of the more recent sea ice data, we focus on results from June 1990 to June 2013.

The carbon cycle component of the CIAO model has been evaluated previously in terms of pCO_2 and pH [*Arrigo and Van Dijken*, 2007; *Arrigo et al*., 2008b; *McNeil et al*., 2010; *Tagliabue and Arrigo*, 2005]. Supporting information Figure S1 compares the interannual variations in total Ross Sea productivity from the model to that derived from satellite data using regionally calibrated algorithms [*Arrigo et al*., 2008a]. This provides confidence in the interannual dynamics produced by the model.

To assess the relative importance of different parameters to the accumulation of anthropogenic carbon, interannual variability in pCO_2, and anthropogenic pCO_2, we used the R package "*relaimpo*" [*Grömping*, 2006] and the metric "LMG" to rank the contribution of each parameter to the total variance explained by the complete linear model. We split our analysis to first focus on the relative roles played by different model forcings (air temperature, specific humidity, precipitation, fractional cloudiness, number of ice-free days, zonal wind speed, and meridional wind speed) and then assess the relative importance of the ocean

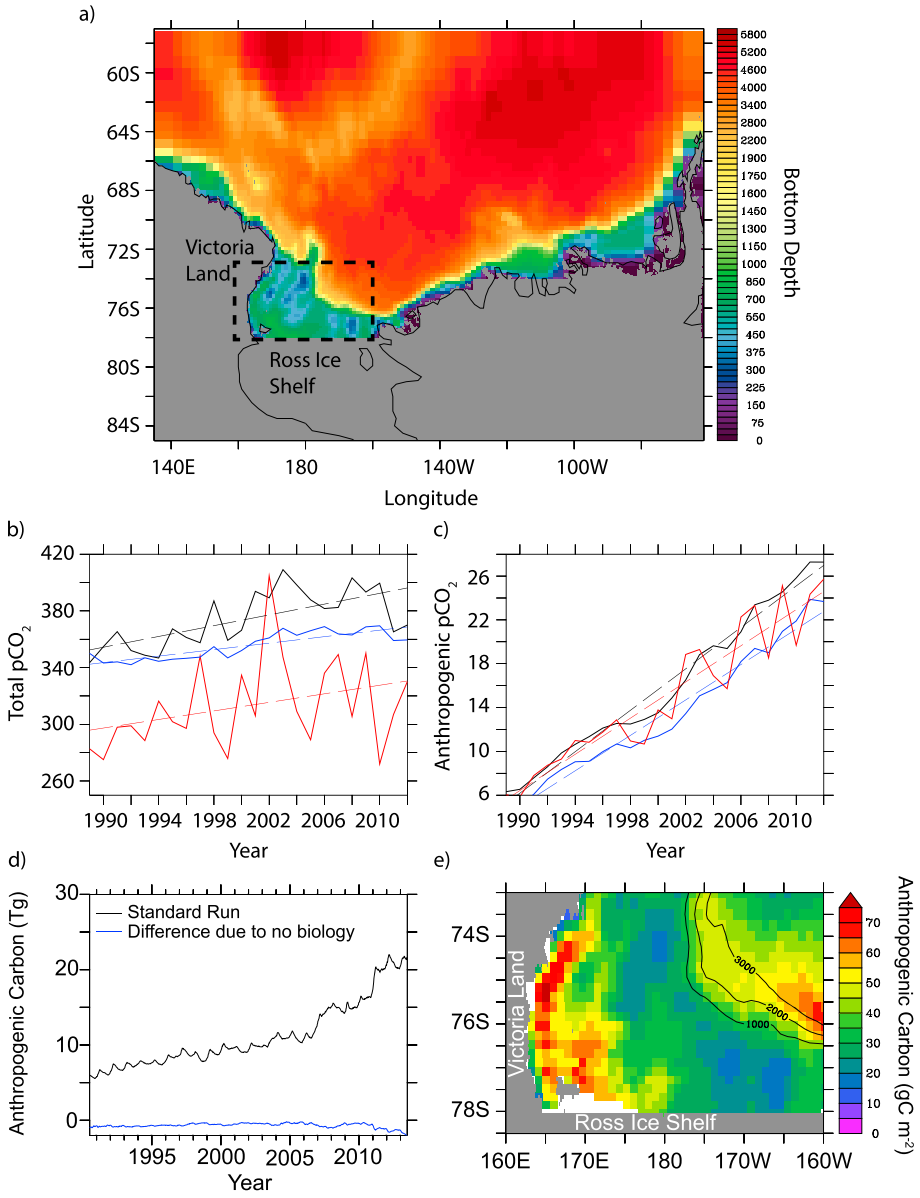

Figure 1. The (a) domain of our model, with the southwestern Ross Sea study area marked with a square, the evolution of annually and spatially averaged (b) total pCO_2 (μatm) and (c) anthropogenic pCO_2 (μatm) over the southwestern Ross Sea. Results and trends from the standard run, without biology and for January only, are represented by black, blue, and red lines, respectively, and dashed lines represent the least squares fit over the period 1990/1991–2011/2012. (d) The evolution of total C_{ant} (Tg C) in the southwestern Ross Sea over the period 1990–2013; the absolute difference when removing biological activity is presented as a blue line. (e) The spatial distribution of C_{ant} (g C m^{-2}) in June 2013 over the southwestern Ross Sea. The 1000, 2000, and 3000 m isobaths are contoured to illustrate the location of the shelf break.

responses that are produced by our model (net primary productivity, sea surface temperature, mixed layer depth, and alkalinity). For the purpose of this study, the southwestern Ross Sea is defined as the region encompassed by 160°E to 170°W and 73°S to the Ross Ice Shelf (Figure 1a). Where described, annual averages are taken across the Austral growing season from June to June.

3. Results and Discussion

3.1. Temporal Trends in pCO_2

Rates of change in pCO_2 have been used previously to assess how the ocean responds to the strong temporal trend in atmospheric CO_2 that arises from anthropogenic emissions. For example, a basin-scale analysis

Table 1. The Rates of Change in pCO_2^{TOTAL} and pCO_2^{ANTH} (Both $\mu atm\ yr^{-1}$) From the Standard Run, the Run With No Biology, and the Rates Extracted From January Only in the Standard Run

	pCO_2^{TOTAL}	pCO_2^{ANTH}
Standard run	1.85 ± 0.72	0.94 ± 0.15
No biology	1.10 ± 0.30	0.80 ± 0.21
January only	1.56 ± 0.92	0.80 ± 0.17

found a pCO_2 growth rate of $2.3 \pm 0.2\ \mu atm\ yr^{-1}$ for the region 45°S–62°S over the period 1995–2008 [*Lenton et al*., 2012]. Rates of change in pCO_2 from our model experiments are summarized in Table 1. Notwithstanding the interannual fluctuations encompassed by the standard deviation, the overall growth rate of annual mean pCO_2 in the Ross Sea ($1.85 \pm 0.72\ \mu atm\ yr^{-1}$, from the standard run, black line in Figure 1a) is within ~20% of the wider Southern Ocean rate and slightly higher than the atmospheric growth rate over the same period ($1.70\ \mu atm\ yr^{-1}$). Removing biology reduces the growth rate by 41% (to $1.10 \pm 0.30\ \mu atm\ yr^{-1}$, blue line in Figure 1b), highlighting the importance of biological activity to the regional-scale trends in total pCO_2. Lastly, the observationally based trends usually rely on summertime measurements in the Southern Ocean [*Lenton et al*., 2012, and references therein] and we find that the January total pCO_2 trend in the Ross Sea from our model is only slightly lower ($1.56 \pm 0.92\ \mu atm\ yr^{-1}$ or within ~15%, red line in Figure 1b) than the full annually averaged model total pCO_2 trend. This suggests that observationally derived trends (which by definition represent total pCO_2) that are based on summertime data will be broadly representative of the annual trend (at least based on the results of our model).

Using our model, we can also isolate the rate of change in anthropogenic pCO_2 (Table 1), which shows a much more consistent trend than total pCO_2 of $0.94 \pm 0.15\ \mu atm\ yr^{-1}$ (from the standard run, black line in Figure 1c). In contrast to total pCO_2, the trend in anthropogenic pCO_2 only changes slightly (to $0.80 \pm 0.21\ \mu atm\ yr^{-1}$ or 15%) when biology is absent (blue line in Figure 1b) due to reduced air-sea gradients in response to the absence of the biological pump. Similar to total pCO_2, the January trend in anthropogenic pCO_2 ($0.80 \pm 0.17\ \mu atm\ yr^{-1}$) is within ~10% of the annual averaged trend (red line in Figure 1c). When compared, the trend in anthropogenic pCO_2 from our model is equivalent to ~50% of the total temporal pCO_2 trend in the Ross Sea (Table 1). Via its impact on pCO_2 trends when it is switched off, our model suggests that biological activity, which has muted influence on anthropogenic pCO_2, plays a more important role in driving total pCO_2 trends.

3.2. Accumulation of Anthropogenic CO_2 in the Southwestern Ross Sea

Over the period 1980–2013, the southwestern Ross Sea took up ~20 Tg of anthropogenic CO_2 from the atmosphere (~0.60 Tg yr^{-1} on average), with modest accumulation rates until 2005 and greater accumulation rates for the last 8 years of the simulation (Figure 1d). The broad trend of anthropogenic carbon (C_{ant}) uptake shows only a slight reduction when biology is absent (Figure 1d) and plays no role in setting the air-sea CO_2 gradient, highlighting the importance of physical processes. Accumulation of C_{ant} results from ocean uptake of atmospheric CO_2 and also physical processes that retain C_{ant} on the shelf. Spatially, depth-integrated inventories of C_{ant} display a heterogeneous pattern over the study region, ranging from ~20 to $>70\ g\ C_{ant}\ m^{-2}$ by 2013 (Figure 1e). We find that C_{ant} is accumulating in the regions closest to Victoria Land and Ross Island and the Ross Ice Shelf, with relatively little C_{ant} accumulating near the shelf break. Our depth-integrated C_{ant} estimates are lower than the range of ~50–300 $g\ C_{ant}\ m^{-2}$ estimated by empirical methods [*Sandrini et al*., 2007] because we only include the C_{ant} taken up since 1980, the date from which the atmospheric forcings necessary to run the model are available.

Due to their variations in space and time, the external forcings of the model (air temperature, specific humidity, precipitation, fractional cloudiness, ice-free days, and zonal and meridional winds) ultimately drive the modeled pattern in C_{ant} accumulation (supporting information Figures S2a–S2g). A linear model including all these external drivers is able to explain 42% of the variance in C_{ant} accumulation and highlights the spatial patterns in zonal winds (UWIND) and to a lesser extent air temperature (T_{AIR}) and specific humidity (Q_{AIR}) as having the highest relative importance (Table 2). When considering the response of the ocean, the full linear model, including net primary productivity (NPP), sea surface temperature (SST), mixed layer depth (MLD), and alkalinity, explains 51% of the variance in C_{ant} accumulation. The highest relative importance is ascribed to NPP, MLD, and, to a lesser extent, alkalinity. Importantly, our analysis suggests that the greatest C_{ant} accumulation is in locations where MLD and alkalinity are high, but NPP is low (Table 2 and supporting information Figures S2h, S2j, and S2k). Conceptually, this implies that greater mixing enhances

Table 2. The Relative Importance of Different Drivers in Explaining the Spatial Patterns in the Accumulation of C_{ant} (C_{ant}) and Interannual Variations in Total pCO_2 (pCO_2^{TOTAL}) and Anthropogenic pCO_2 (pCO_2^{ANTH})[a]

	Metric		
Driver	C_{ant}	pCO_2^{TOTAL}	pCO_2^{ANTH}
T_{AIR}	0.19	−0.31	0.08
Q_{AIR}	−0.19	−0.32	−0.13
QINT	0.11	−0.08	0.16
CLDF	−0.05	−0.02	−0.08
IFD	−0.15	0.05	0.11
UWIND	0.23	−0.16	0.34
VWIND	−0.09	0.06	0.08
R^2	0.42	0.63	0.24
NPP	−0.52	0.46	0.01
SST	−0.09	0.02	0.57
MLD	0.24	0.11	−0.39
ALK	0.14	0.41	0.03
R^2	0.51	0.31	0.17

[a]The roles of external forcings, air temperature (T_{AIR}), specific humidity (Q_{AIR}), precipitation (QINT), fractional cloudiness (CLDF), ice-free days (IFD), zonal winds (UWIND), and meridional winds (VWIND), are considered independent of "ocean properties": net primary production (NPP), mixed layer depth (MLD), sea surface temperature (SST), and alkalinity (ALK). The bottommost row indicates the R^2 associated with the full linear model for each suite of drivers, and there are 660 observations in each case.

C_{ant} storage via subduction and increased alkalinity drives enhanced air-sea pCO_2 gradients via carbon chemistry. Overall, as we find no link to elevated NPP (the biological pump), our model suggests a key role for the role of the solubility pump (via zonal winds impacting the MLD), with a smaller role for carbonate chemistry, in driving the accumulation of C_{ant} in the southwestern Ross Sea.

3.3. Spatial and Temporal Anomalies in Total and Anthropogenic pCO_2

It is notable that we found no links between annual and spatial mean anomalies and the SAM, a climate index that dominates Southern Ocean variability, similar to recent Southern Ocean CO_2 trends [*Landschutzer et al.*, 2015]. Specifically, the SAM explains only around 4% of the variance in both total pCO_2 and anthropogenic pCO_2 anomalies (which are more closely linked to changes in productivity and mixing). Similarly, while global climate models find a strong link to the SAM in the sub-Antarctic waters of the Southern Ocean, convective processes are found to be more important in the Antarctic region [*Resplandy et al.*, 2015] (biological activity on the shelf is not well represented by such coarse resolution models). Ultimately, the mechanisms underlying the spatial mean drivers in the Ross Sea are difficult to isolate in our model due to the strong spatial gradients in the potential driving factors over the region (supporting information Figures S2 and S3).

To further examine the spatial variations in pCO_2, we computed anomalies (relative to the long-term trend) in total pCO_2 and anthropogenic pCO_2 over the period 1990–2013 specific to each model grid cell and then used the standard deviation as an index of the strength of interannual variability (Figures 2a and 2b). The highest rates of interannual variability were spatially distinct, with the largest anomalies located in a broad region of the central Ross Sea and restricted to the continental shelf break for pCO_2 and anthropogenic pCO_2, respectively (Figures 2a and 2b). It is notable that although absolute anomalies in total pCO_2 were much larger than those for anthropogenic pCO_2, each represents around 10% or 10–20% of total pCO_2 and anthropogenic pCO_2, respectively.

The strongest external drivers of the modeled variability in total pCO_2 from a full linear model that explains 63% of the variance in total pCO_2 anomalies were identified as anomalies in T_{AIR} and Q_{AIR}, with a lesser role for zonal winds (Table 2). The impact on anomalies in total pCO_2 clearly manifested itself due to variations in NPP and alkalinity, which both had the highest relative importance (Table 2; the full linear model explains 31% of the variance in total pCO_2). A parallel analysis showed that the anomalies in NPP were driven primarily by Q_{AIR} and zonal winds, while variations in alkalinity were caused by T_{AIR}. This highlights the importance of the spatial variability in this suite of drivers in controlling the patterns of total pCO_2 interannual variability, which itself was greatest over a wide geographic area (Figure 2a). The variability in anthropogenic pCO_2 was more spatially localized (Figure 2b) than total pCO_2 and was more closely linked to anomalies in zonal winds (with Q_{AIR}, precipitation and sea ice playing small roles) that then affected SST and, to a lesser extent, MLD (Table 2). It is notable that the full linear model for external drivers and ocean processes can only explain 24% and 17% of the variance in anthropogenic pCO_2, respectively, which implies a role for alternative processes not considered in our analysis. For example, if interactions between the atmospheric drivers are included, then over 80% of the variance in anthropogenic pCO_2 can be accounted for (interactions between

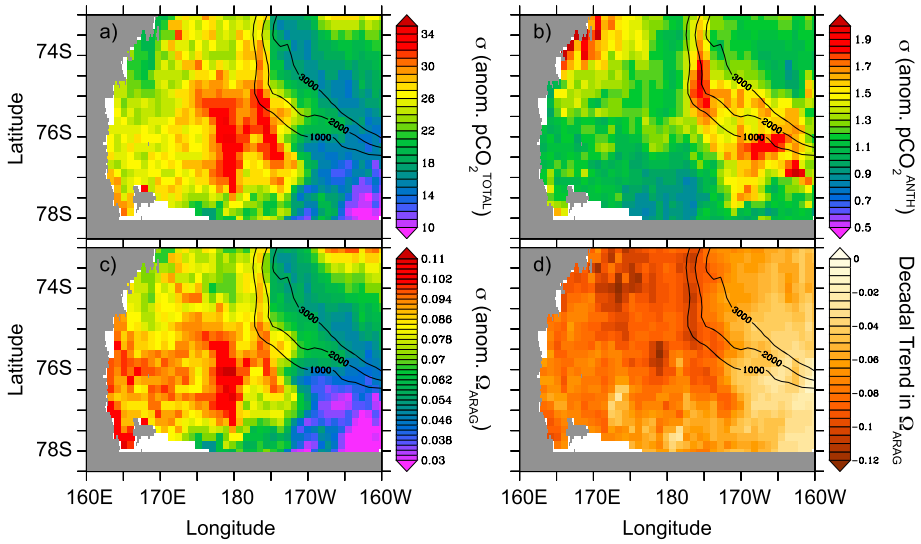

Figure 2. The distributions of the anomalies in annually averaged (a) total pCO_2 (μatm) and (b) anthropogenic pCO_2 (μatm) as well as (c) anomalies in aragonite saturation and (d) its decadal trend. The 1000, 2000, and 3000 m isobaths are contoured to illustrate the location of the shelf break.

T_{AIR}, precipitation (QINT), fractional cloudiness (CLDF), and meridional wind (VWIND) emerge as some of the more important). Focusing on the results of the noninteractive models, we find that while the solubility pump again emerges as important for anthropogenic pCO_2, the interannual variability in total pCO_2 is more closely linked to the biological pump and carbon chemistry (via the important roles we find for NPP and alkalinity).

4. Wider Implications

At the scale of the southwestern Ross Sea, we found that the growth rate in pCO_2 of 1.85 ± 0.72 μatm yr^{-1} was within 20% of that estimated for offshore regions of the Southern Ocean (2.3 ± 0.2 μatm yr^{-1}) [*Lenton et al.*, 2012], although it displayed around threefold more variability. This highlights the presence of strong spatial extremes in the pCO_2 trends that can be important when considering, for example, ocean acidification impacts (rates of change in pH and pCO_2 are strongly anticorrelated, $R^2 = 0.99$). Accordingly, some regions of the Ross Sea may experience stronger than average rates of acidification, with consequences for thresholds in the saturation state of aragonite (Ω_{ARAG}) and calcite.

The fluctuations in pCO_2 we found may impact the success of the aragonite-producing pteropod *Limacina helicina*, which is an important component of the Ross Sea zooplankton community [*Hunt et al.*, 2008; *Seibel and Dierssen*, 2003]. *L. helicina* has also been observed to contribute significantly to the regional flux of both carbonate and organic carbon [*Collier et al.*, 2000], and its shell production is sensitive to low pH due to reduced calcium carbonate precipitation rates [*Comeau et al.*, 2010]. We computed Ω_{ARAG} based on modeled temperature, salinity, total CO_2, and pH using standard CO_2 dissociation constants [*Dickson and Millero*, 1987] and calculated interannual anomalies (with the long-term trend removed, Figure 2c). At most Ω_{ARAG} shows variability of over 0.1 units over a relatively large region (Figure 2c), with high Ω_{ARAG} anomalies in the central Ross Sea reflecting similar variations in total pCO_2 (Figure 2a) and those closest to Victoria Land linked to alkalinity (supporting information Figure S3k). Interestingly, the degree of interannual variability we find for Ω_{ARAG} at local scales is of the same order as the long-term decadal Ω_{ARAG} trend (Figure 2d). Taken together, this implies that aragonite-producing members of the Ross Sea ecosystem will be affected by a combination of the long-term "anthropogenic" trend, alongside high levels of interannual variability at local scales.

Our analysis emphasizes that variations in carbon cycle of the Ross Sea over space and time are likely to be strongly regional and more closely linked to episodic events rather than larger-scale phenomena or trends. For example, we found that anthropogenic CO_2 trends (that reflect long-term atmospheric CO_2 accumulation) were equivalent to around half of the total pCO_2 trends and broad-scale drivers like the SAM had little

predictive power for the modeled pCO_2 trends. That our mean total pCO_2 trend over the entire region matches estimates from the wider Southern Ocean suggests a link to larger-scale processes, although our model produces >3 times greater variability within the Ross Sea. We have identified how variations in air temperature, specific humidity, and zonal winds drive the anomalies in total pCO_2 (that might be observed) via their influence on NPP and alkalinity. These properties show strong regionality over the study area (supporting information Figure S2), linked to fluctuations in sea-ice dynamics and local katabatic winds [*Comiso et al*., 2011; *Smith et al*., 2014b], which then regulate the momentum and buoyancy fluxes that govern local MLD, nutrient fluxes, and NPP. Ultimately, this heterogeneity will make identifying regional-scale constraints on the spatiotemporal trends in the carbon cycle of the southwestern Ross Sea from observations challenging. As the Ross Sea is not unusual, relative to other polynya systems on the Antarctic shelf, in being influenced by local wind and sea ice conditions [*Arrigo et al*., 2015], we expect the roles we find for physical, chemical, and biological processes in influencing the carbon cycle to be widespread.

Models are useful tools for extrapolating the wider spatial and temporal scales and for testing hypotheses, but they rely on assumptions that should be continuously reassessed. For example, in our analysis, alkalinity emerged as an important driver in this region (Table 2), but we do not include calcification/dissolution processes explicitly in our model [*Tagliabue and Arrigo*, 2005], relying instead on an established empirical relationship to physical variables [*Lee et al*., 2006]. In the future, it would be useful to explore the influence of an active contribution of pteropods (as members of the zooplankton community) to the alkalinity budget in the model toward a full description of alkalinity sources and sinks. This would enable an assessment as to the impact of local extremes in acidification on the zooplankton community, which may then affect the degree of phytoplankton-zooplankton coupling. Although our physical model is much higher resolution than those used to explore regional-scale Southern Ocean carbon cycling [e.g., *Lenton et al*., 2009], it remains coarser than other models that assess the physical oceanography of the Ross Sea [*Dinniman et al*., 2011; *Smith et al*., 2014a]. However, due to computational expense, these high-resolution model exercises are unable to explicitly assess biogeochemical-carbon cycle interactions that are the focus of this study. One potentially important shortcoming of our model is our reliance on imposed sea ice [*Arrigo et al*., 2003]. While this has the advantage of ensuring that the model reproduces observed sea ice dynamics, it might not properly represent the interactions between changing wind patterns, ice advection, and the associated impacts on freshwater fluxes.

5. Conclusions

We used a regional model of the southwestern Ross Sea to diagnose the trends and drivers behind variability in the carbon cycle. We found that the accumulation of C_{ant} on the shelf was restricted to specific regions that are typified by low productivity and deep mixing forced by zonal winds. Trends in total pCO_2 are strongly affected by biological activity, and anthropogenic pCO_2 is equivalent to approximately half of the total trend. Regionally varying signatures of the impact of specific humidity and zonal winds on NPP and air temperature on alkalinity regulate interannual variations in total pCO_2. Conversely, the year-to-year fluctuations in anthropogenic pCO_2 are caused by the impact of variations in zonal winds on SST and to a lesser extent MLD. We find a large degree of spatial variability in the magnitude of the trends in pCO_2, with potentially important implications for ocean acidification at local scales via changes in aragonite saturation. Overall, the Ross Sea emerges as a strongly regional system, controlled by multiple local processes rather than larger-scale phenomena (such as climate modes or growth rates of atmospheric CO_2).

Acknowledgments
We used NCEP_Reanalysis 2 data provided by the NOAA/OAR/ESRL PSD, Boulder, Colorado, USA, from their Web site at http://www.esrl.noaa.gov/psd. We thank two anonymous reviewers for their constructive comments on our manuscript. Model output is available upon request to A.T.

References

Arrigo, K. R., and G. L. van Dijken (2003), Phytoplankton dynamics within 37 Antarctic coastal polynya systems, *J. Geophys. Res.*, *108*(C8), 3271, doi:10.1029/2002JC001739.

Arrigo, K. R., and G. L. van Dijken (2004), Annual changes in sea-ice, chlorophyll *a*, and primary production in the Ross Sea, Antarctica, *Deep Sea Res., Part II*, *51*(1–3), 117–138, doi:10.1016/j.dsr2.2003.04.003.

Arrigo, K. R., and G. L. Van Dijken (2007), Interannual variation in air-sea CO_2 flux in the Ross Sea, Antarctica: A model analysis, *J. Geophys. Res.*, *112*, C03020, doi:10.1029/2006JC003492.

Arrigo, K. R., D. L. Worthen, and D. H. Robinson (2003), A coupled ocean-ecosystem model of the Ross Sea: 2. Iron regulation of phytoplankton taxonomic variability and primary production, *J. Geophys. Res.*, *108*(C7), 3231, doi:10.1029/2001JC000856.

Arrigo, K. R., G. L. van Dijken, and S. Bushinsky (2008a), Primary production in the Southern Ocean, 1997–2006, *J. Geophys. Res.*, *113*, C08004, doi:10.1029/2007JC004551.

Arrigo, K. R., G. van Dijken, and M. Long (2008b), Coastal Southern Ocean: A strong anthropogenic CO_2 sink, *Geophys. Res. Lett.*, *35*, L21602, doi:10.1029/2008GL035624.

Arrigo, K. R., G. L. van Dijken, and A. L. Strong (2015), Environmental controls of marine productivity hot spots around Antarctica, *J. Geophys. Res. Oceans*, *120*, 5545–5565, doi:10.1002/2015JC010888.

Blumberg, A. F., and G. L. Mellor (1987), A description of a three-dimensional coastal ocean circulation model, in *Three-Dimensional Coastal Ocean Models*, vol. 4, pp. 1–16, AGU, Washington, D. C., doi:10.1029/CO004p0001.

Collier, R., J. Dymond, S. Honjo, S. Manganini, R. Francois, and R. Dunbar (2000), The vertical flux of biogenic and lithogenic material in the Ross Sea: Moored sediment trap observations 1996–1998, *Deep Sea Res., Part II*, *47*(15–16), 3491–3520, doi:10.1016/S0967-0645(00)00076-X.

Comeau, S., R. Jeffree, J. L. Teyssie, and J. P. Gattuso (2010), Response of the Arctic pteropod Limacina helicina to projected future environmental conditions, *PLoS One*, *5*(6), e11362, doi:10.1371/journal.pone.0011362.

Comiso, J. C., R. Kwok, S. Martin, and A. L. Gordon (2011), Variability and trends in sea ice extent and ice production in the Ross Sea, *J. Geophys. Res.*, *116*, C04021, doi:10.1029/2010JC006391.

Dickson, A. G., and F. J. Millero (1987), A comparison of the equilibrium constants for the dissociation of carbonic acid in seawater media, *Deep Sea Res., Part A*, *34*(10), 1733–1743, doi:10.1016/0198-0149(87)90021-5.

Dinniman, M. S., J. M. Klinck, and W. O. Smith (2011), A model study of circumpolar deep water on the West Antarctic Peninsula and Ross Sea continental shelves, *Deep Sea Res., Part II*, *58*(13-16), 1508–1523, doi:10.1016/j.dsr2.2010.11.013.

Dlugokencky, E., and P. Tans (2013), NOAA/ESRL. [Available at http://www.esrl.noaa.gov/gmd/ccgg/trends/].

Dunbar, R. B., A. R. Leventer, and D. A. Mucciarone (1998), Water column sediment fluxes in the Ross Sea, Antarctica: Atmospheric and sea ice forcing, *J. Geophys. Res.*, *103*, 30,741–30,759, doi:10.1029/1998JC900001.

Gordon, A. L., E. Zambianchi, A. Orsi, M. Visbeck, C. F. Giulivi, T. Whitworth III, and G. Spezie (2004), Energetic plumes over the western Ross Sea continental slope, *Geophys. Res. Lett.*, *31*, L21302, doi:10.1029/2004GL020785.

Grömping, U. (2006), Relative importance for linear regression in R: The package relaimpo, *J. Stat. Software*, *17*(1), 1–27.

Hunt, B. P. V., E. A. Pakhomov, G. W. Hosie, V. Siegel, P. Ward, and K. Bernard (2008), Pteropods in Southern Ocean ecosystems, *Prog. Oceanogr.*, *78*(3), 193–221, doi:10.1016/j.pocean.2008.06.001.

Khatiwala, S., F. Primeau, and T. Hall (2009), Reconstruction of the history of anthropogenic CO_2 concentrations in the ocean, *Nature*, *462*(7271), 346–349, doi:10.1038/nature08526.

Landschutzer, P., et al. (2015), The reinvigoration of the Southern Ocean carbon sink, *Science*, *349*(6253), 1221–1224, doi:10.1126/science.aab2620.

Lee, K., L. T. Tong, F. J. Millero, C. L. Sabine, A. G. Dickson, C. Goyet, G.-H. Park, R. Wanninkhof, R. A. Feely, and R. M. Key (2006), Global relationships of total alkalinity with salinity and temperature in surface waters of the world's oceans, *Geophys. Res. Lett.*, *33*, L19605, doi:10.1029/2006GL027207.

Lenton, A., F. Codron, L. Bopp, N. Metzl, P. Cadule, A. Tagliabue, and J. Le Sommer (2009), Stratospheric ozone depletion reduces ocean carbon uptake and enhances ocean acidification, *Geophys. Res. Lett.*, *36*, L12606, doi:10.1029/2009GL038227.

Lenton, A., N. Metzl, T. Takahashi, M. Kuchinke, R. J. Matear, T. Roy, S. C. Sutherland, C. Sweeney, and B. Tilbrook (2012), The observed evolution of oceanic pCO_2 and its drivers over the last two decades, *Global Biogeochem. Cycles*, *26*, GB2021, doi:10.1029/2011gb004095.

Le Quere, C., et al. (2007), Saturation of the Southern Ocean CO_2 sink due to recent climate change, *Science*, *316*(5832), 1735–1738, doi:10.1126/science.1136188.

Martin, S., R. S. Drucker, and R. Kwok (2007), The areas and ice production of the western and central Ross Sea polynyas, 1992–2002, and their relation to the B-15 and C-19 iceberg events of 2000 and 2002, *J. Mar. Syst.*, *68*(1–2), 201–214, doi:10.1016/j.jmarsys.2006.11.008.

McNeil, B. I., A. Tagliabue, and C. Sweeney (2010), A multi-decadal delay in the onset of corrosive "acidified" waters in the Ross Sea of Antarctica due to strong air-sea CO_2 disequilibrium, *Geophys. Res. Lett.*, *37*, L19607, doi:10.1029/2010GL044597.

Mellor, G. L., and T. Yamada (1982), Development of a turbulence closure model for geophysical fluid problems, *Rev. Geophys.*, *20*, 851–875, doi:10.1029/RG020i004p00851.

Orr, J. C., et al. (2005), Anthropogenic ocean acidification over the twenty-first century and its impact on calcifying organisms, *Nature*, *437*(7059), 681–686, doi:10.1038/nature04095.

Peng, G., W. N. Meier, D. J. Scott, and M. H. Savoie (2013), A long-term and reproducible passive microwave sea ice concentration data record for climate studies and monitoring, *Earth Syst. Sci. Data*, *5*(2), 311–318, doi:10.5194/essd-5-311-2013.

Resplandy, L., R. Séférian, and L. Bopp (2015), Natural variability of CO_2 and O_2 fluxes: What can we learn from centuries-long climate models simulations? *J. Geophys. Res. Oceans*, *120*, 384–404, doi:10.1002/2014JC010463.

Sallée, J.-B., R. J. Matear, S. R. Rintoul, and A. Lenton (2012), Localized subduction of anthropogenic carbon dioxide in the Southern Hemisphere oceans, *Nat. Geosci.*, *5*(8), 579–584, doi:10.1038/ngeo1523.

Sandrini, S., N. Ait-Ameur, P. Rivaro, S. Massolo, F. Touratier, L. Tositti, and C. Goyet (2007), Anthropogenic carbon distribution in the Ross Sea, Antarctica, *Antarct. Sci.*, *19*(03), 395, doi:10.1017/s0954102007000405.

Schine, C. M. S., G. van Dijken, and K. R. Arrigo (2016), Spatial analysis of trends in primary production and relationship with large-scale climate variability in the Ross Sea, Antarctica (1997–2013), *J. Geophys. Res. Oceans*, *121*, 368–386, doi:10.1002/2015JC011014.

Seibel, B. A., and H. M. Dierssen (2003), Cascading trophic impacts of reduced biomass in the Ross Sea, Antarctica: Just the tip of the iceberg? *Biol. Bull.*, *205*(2), 93–97, doi:10.2307/1543229.

Smith, W. O., Jr., M. S. Dinniman, E. E. Hofmann, and J. M. Klinck (2014a), The effects of changing winds and temperatures on the oceanography of the Ross Sea in the 21st century, *Geophys. Res. Lett.*, *41*, 1624–1631, doi:10.1002/2014GL059311.

Smith, W. O., Jr., D. G. Ainley, K. R. Arrigo, and M. S. Dinniman (2014b), The oceanography and ecology of the Ross Sea, *Annu. Rev. Mar. Sci.*, *6*, 469–487, doi:10.1146/annurev-marine-010213-135114.

Stammerjohn, S. E., D. G. Martinson, R. C. Smith, X. Yuan, and D. Rind (2008), Trends in Antarctic annual sea ice retreat and advance and their relation to El Niño–Southern Oscillation and Southern Annular Mode variability, *J. Geophys. Res.*, *113*, C03S90, doi:10.1029/2007JC004269.

Sweeney, C. (2003), The annual cycle of surface water CO_2 and O_2 in the Ross Sea: A model for gas exchange on the continental shelves of Antarctica, in *Biogeochemistry of the Ross Sea*, vol. 78, pp. 295–312, AGU, Washington, D. C., doi:10.1029/078ars19.

Tagliabue, A., and K. R. Arrigo (2005), Iron in the Ross Sea: 1. Impact on CO_2 fluxes via variation in phytoplankton functional group and non-Redfield stoichiometry, *J. Geophys. Res.*, *110*, C03009, doi:10.1029/2004JC002531.

Volk, T., and M. I. Hoffert (1985), Ocean carbon pumps: Analysis of relative strengths and efficiencies in ocean-driven atmospheric CO_2 changes, in *The Carbon Cycle and Atmospheric CO_2: Natural Variations Archean to Present*, pp. 99–110 , AGU, Washington, D. C.

Zeebe, R. E., and D. A. Wolf-Gladrow (2001), *CO_2 in Seawater: Equilibrium, Kinetics, Isotopes*, Elsevier Oceanogr. Ser., Amsterdam.